

Large-Scale Vine Robots for Industrial Inspection

Developing a New Framework to Overcome Limitations With Existing Inspection Methods

By William E. Heap^{ID}, Steven Man^{ID},
Vedad Bassari, Steven Nguyen^{ID},
Elvy B. Yao^{ID}, Neel A. Tripathi^{ID},
Nicholas D. Naclerio^{ID}, and
Elliot W. Hawkes^{ID}

Industrial facilities such as chemical factories, gas terminals, and power plants can contain kilometers of piping that require meticulous inspection for leaks and defects prior to operation. This is a costly and time-consuming process that sometimes requires dismantling sections of pipe. While current internal inspection devices such as borescopes, “pipe inspection gadgets,” rovers, and drones serve specific purposes, none can effectively maneuver through multiple bends with large diameter changes while pulling a tethered sensor. As a first step in addressing this need, we tackled the mobility challenge without a sensor, developing a 33-m-long, 1-m-wide, soft, inflatable vine robot for accessing hard-to-reach spaces in dangerous industrial facilities. We also investigated ways to mount sensors to large-scale vine robots, identified key challenges in doing so, and provide the framework for a potential solution. Our work addresses many modeling, design, and scaling challenges, including frictional properties, gravitational effects, pneumatic control, and portability. To validate the device’s capabilities, we conducted testing at a Bechtel facility in Houston, TX, USA. Our portable device successfully navigated a 24-m-long section of oil and gas piping, negotiating a 90° bend, a vertical section, a block-

age, and an open chamber. Our work not only represents a substantial advancement in addressing current pipe navigation challenges but also establishes a new benchmark as the world’s largest soft robot, showcasing the effectiveness of pneumatic principles at large scales.

©SHUTTERSTOCK.COM/ADAM VILIMEK



Digital Object Identifier 10.1109/MRA.2024.3487326
Date of publication 20 November 2024;
date of current version 11 September 2025.

INTRODUCTION

Industrial facilities, including chemical plants, natural gas terminals, and power plants, contain critical equipment and infrastructure that require regular inspection. The frequency and cost of these inspections can be high due to industrial facilities’ large scales, expensive equipment and products, and potential safety hazards for inspectors and society at large. To reduce the costs and risks associated with inspections, robots can be used to replace human inspectors and provide new inspection modalities [1].

However, a significant difficulty for inspection robots is accessing large-scale spaces with restricted entrances or passageways. This can include equipment such as large storage tanks with centimeter-scale openings or tall chemical distillation towers with complex interiors. A particular challenge is industrial pipe systems, which can be hundreds of meters long with turns, vertical sections, and large changes in diameter. An example of a shorter section of process piping with a robot for internal inspection is shown in Figure 1. While external inspection methods exist, they are often inadequate, and instead, sensors must be transported through the pipe. Doing so is a design challenge as the length, verticality, and tortuosity of industrial pipe systems limit the mobility of tethered robots. While untethered robots may have improved mobility, they have limited live data transmission ranges and operating times. As an added complexity, pipe systems with large changes in diameter, such as a pipe leading to a storage tank, prevent common robotic locomotion methods. This leads to an unsolved challenge in robotics: Can a tethered robot traverse a long and tortuous pipe system with large changes in diameter?

Bechtel, a large engineering and construction firm, faced this challenge while inspecting new liquid natural gas (LNG) plants and pipelines. LNG plants can process tens of millions of tons of LNG per year, but before they can go into operation, their kilometers of piping must be inspected for any leaks or defects [2]. Despite both purchasing commercially available robots and fabricating robots in-house, Bechtel was unable to develop a nondestructive solution. Instead, Bechtel breaks apart pipe systems so current inspection methods can be used on shorter lengths of pipe.

Four internal pipe inspection methods are primarily used commercially: borescopes, pipe inspection gadgets (PIGs), rovers, and drones. Each method works well in a subset of pipe configurations, but none can be used universally [3].

This is because these four common devices are limited by their propulsion methods. Borescopes must be pushed from the entrance of the pipe, which leads to friction buildup and kinking. PIGs require a pressurized fluid to propel them, restricting them to pipes with limited changes in diameter. Rovers using wheels, rollers, or inchworm locomotion rely on frictional or magnetic contacts, limiting the pipe materials and geometries they can operate in. Finally, drones’ propeller-based propulsion allows them to navigate areas with significant diameter increases, but their propulsion force is very limited and prevents them from pulling a tether through tortuous paths.

Here, we propose a solution to Bechtel’s challenge and the limitations of current inspection devices: a large-scale vine-inspired robot that utilizes a unique propulsion method of pressure-driven tip extension. Pressure-driven tip extension

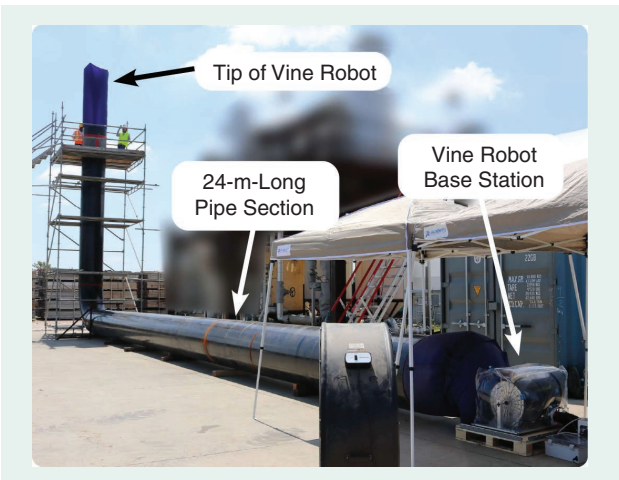


FIGURE 1. The vine robot growing through a 24-m-long test pipe system with a 90° bend and emerging 3 m out of the pipe in the top left of the image next to two researchers. The background of the image is blurred to protect confidential Bechtel Corporation equipment.



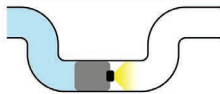
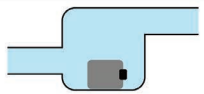
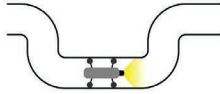





Inspection Method	Ideal For	Limited By
Borescope	 <ul style="list-style-type: none">• Small Bore Pipes With Minimal Turns	 <ul style="list-style-type: none">• Tortuous Pipe System With Large Bore Pipe and Open Areas
Pipe Inspection Gauge	 <ul style="list-style-type: none">• Long Pipe Systems• Not Interrupting Service	 <ul style="list-style-type: none">• Large Changes in Diameter• Requires Flow
Rover	 <ul style="list-style-type: none">• Long and Tortuous Pipes	 <ul style="list-style-type: none">• Tethered in Nonmagnetic Tortuous Pipes With Large Diameter Change
Drone	 <ul style="list-style-type: none">• Large Changes in Pipe Diameter With Minimal Turns	 <ul style="list-style-type: none">• Long and Tortuous Paths
Vine Robot	 <ul style="list-style-type: none">• Long and Tortuous Paths With Large Changes in Diameter	 <ul style="list-style-type: none">• Yet to be Demonstrated at Large Scale

FIGURE 2. Four current pipe inspection methods and their limitations. The fifth inspection method, the vine robot, utilizes a unique operating principle that allows for the inspection of pipe networks that are inaccessible to existing instruments.

TABLE 1. End user inspection needs as specified by Bechtel along with the corresponding engineering requirements and the selected solutions. The focus of our work was the navigation and job-site deployment end-user needs, and their corresponding requirements.

END USER NEEDS	SPECIFIC REQUIREMENTS	SOLUTIONS
Navigation of pipe system	The robot must travel through a 49-m (163-ft)-long pipe featuring a 90° elbow and open chamber	Large-scale lightweight pneumatic vine robot Teleoperated control
	The robot must reach the end of the pipe system in under 20 min	Operation modeling to inform motor and fan selection
Inspection inside of the pipe system	Real-time video feed to the operator Hard-wired communication with the operator	Custom communication system with wired and wireless subsystems
Job-site deployment	Each component must weigh fewer than 22.5 kg (50 lb)	Compact modular design of base station components
	Each component must have one linear dimension fewer than 0.9 m (3 ft)	
	The robot must be robust to dirt, debris, and high temperatures inside the pipe Physical tether to robot	Durable low-friction silicone-coated fabric robot body Internal fabric tail of the robot used as a physical tether

provides vine robots with several inherent advantages over borescopes, PIGs, rovers, and drones. Most significantly, vine robots can generate substantial propulsion forces independent of environmental interactions. Vine robots are also soft and compliant and do not translate relative to their environment. Instead, as their tip extends, vine robots create a continuously lengthening self-supporting body that can be steered in free space or confined areas. These capabilities allow vine robots to navigate fragile, debris-filled, long, and tortuous paths with large changes in diameter, whereas existing commercial solutions are limited by one or multiple factors (Figure 2).

Inspired by our past work on small-scale tip-extending devices, Bechtel contacted us for a partnership and provided us with real-world design constraints, including a test segment of pipe system similar to the ones they were unable to inspect with existing robots. While our work focused on developing a robot for pipe inspection, we believe vine robots' unique capabilities make them broadly applicable to the inspection of large-scale spaces with restricted access points or confined passageways. Thus, our goals were twofold: 1) to build a vine robot system

that demonstrates the applicability of large-scale vine robots to improve accessibility within a wide variety of large-scale industrial facilities and 2) to meet the mobility and portability requirements imposed by Bechtel for inspecting a test pipe system (Table 1). In doing so, we designed and built a vine robot an order of magnitude larger than any previous work [4], and, to the best of our knowledge, the largest soft robot to date [5].

In this article, we will discuss the following:

- the background, including design requirements for large-scale pipe inspection and a review of vine robots as they relate to inspection
- an analytical model and design tool for vine robot operation in an arbitrary pipe system
- the design of a large-scale vine robot for in-pipe navigation
- preliminary results on a method to mount sensors to large-scale vine robots
- the results from the deployment of the large-scale pipe-inspection vine robot at Bechtel's testing facility in Houston, TX, USA.

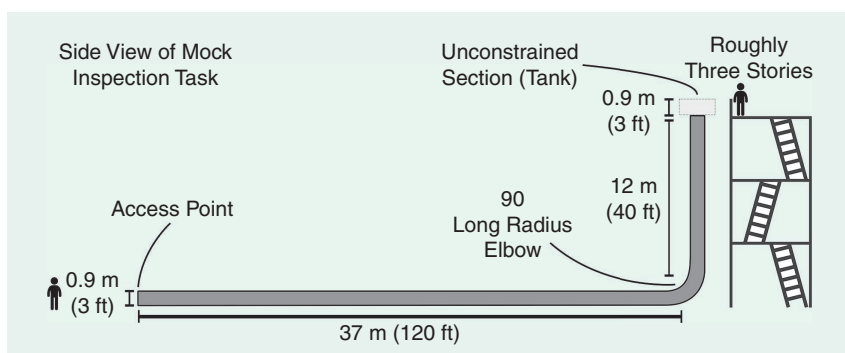


FIGURE 3. A diagram of the pipe network specified by Bechtel for the mock inspection task. The unconstrained section at the end of the pipe simulates a sudden increase in pipe diameter.

BACKGROUND: TASK REQUIREMENTS AND VINE ROBOTS

PIPE INSPECTION TASK REQUIREMENTS

Bechtel provided an important pipe system inspection scenario (shown in Figure 3) for which none of the current technologies offer solutions. The eventual goal is for a robot to traverse a 37-m (120-ft)-long, 0.9-m (3-ft)-diameter horizontal segment of steel pipe followed by a 90° bend, a 12-m

(40-ft) vertical segment, and finally, 0.9 m (3 ft) of an open chamber, simulating a holding tank, in under 20 min while providing live video of the pipe interior through wired data transfer. Additional requirements from Bechtel (listed in Table 1) are to ensure durability in the 35 °C Texas heat, follow Occupational Safety and Health Administration (OSHA) regulations [6], and ensure ease of use and transport in field conditions. As a first step toward addressing the full challenge, we focused on meeting the navigation and job-site deployment requirements. We also conducted the preliminary development of a sensor mount and communications system to gain insight into meeting the inspection requirements.

This inspection scenario represents LNG process piping, which can span hundreds of meters in length to transport LNG from ships to holding tanks. Depending on the facility, pipelines can contain multiple 90° bends, vertical sections, and increased diameter sections containing valves or other equipment. Some key inspection needs for these pipe systems include verifying the weld quality between pipe sections, ensuring that no foreign object debris has been left in the line, and checking that valves are operating as intended.

VINE ROBOT BACKGROUND

Vine robots have been broadly researched to leverage their ability to navigate through cluttered and highly constrained environments [7], [8], [9], [10], [11]. As illustrated in Figure 4, vine robots consist of a thin tube of film or fabric inverted into itself such that when the tube is pressurized, the inverted material everts from the tip of the robot. Conversely, retracting the inverted material causes inversion and shortening at the robot's tip. This continuous lengthening from its tip creates plant-like growth without the complexity of biological growth.

Tip extension allows vine robots to navigate traditionally challenging environments. As there is no relative movement between the robot's skin and its environment, vine robots can squeeze through sharp, sticky, and tortuous obstacles. Meanwhile, the compliance of pneumatic vine robots allows them to passively turn, actively steer, and grow through gaps smaller than their diameter [10]. These capabilities are useful for navigating pipe system features, including sharp turns, branches, and constrictions.

Vine robots are specifically well suited for pipe inspection for two additional reasons. First, their pressure-driven eversion allows them to generate significant propulsion forces to clear blockages and pull a tether through a long and tortuous path. Second, as the vine robot grows through a pipe, it creates a continuous body to support itself and sensors in free space. This continuous body can also generate significant frictional forces with the environment, reducing or removing the need for reaction forces at the base of the vine robot. That is, the tip of the vine robot can push with a much larger force than the product of its base weight and the coefficient of friction. Due to their

advantages in navigation, numerous vine robot systems have been constructed for applications, including archaeology [12], coral reef exploration [13], and disaster area searches [4].

Vine robot systems generally consist of the following subcomponents [7]:

- 1) the inflated vine robot body and deflated internal tail that hold the pneumatic pressure of the robot and enable growth and retraction
- 2) a motorized spool that winds the vine robot material to control growth and retraction rates and compactly store the predeployed robot
- 3) a stationary base station from which the robot grows, holding the motorized spool, pneumatic supply, and control system
- 4) a camera or sensor mount attached to the continuously everting tip of the robot to transmit information back to the base station.

LIMITATIONS OF CURRENT VINE ROBOTS

The challenge posed by Bechtel prevented previous vine robot designs from being used, requiring new designs, for the following reasons:

- The challenge required a vine robot to perform self-supported and environmentally supported vertical growth at

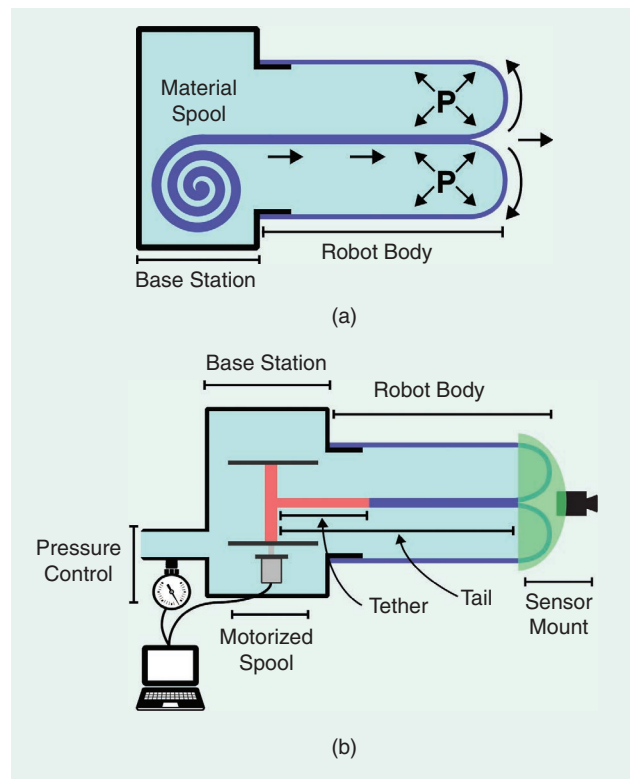


FIGURE 4. An overview of the working principle of vine robots. (a) Growth is achieved by pressurizing the robot's body while retraction is accomplished by pulling the robot's tail. (b) A common configuration for vine robots enabling user-controlled growth, retraction, and sensor deployment. (a) Vine robot working principle. (b) Common vine robot implementation.

the meter scale, neither of which has been previously demonstrated.

- The challenge led to a vine robot with a diameter eight times larger (91 cm versus 11 cm) and a length two times longer (33 m versus 17 m) than any prior work, resulting in an overall surface area increase of more than 50× [4], [14]. Such a massive upscaling resulted in the need for fundamentally different solutions. For instance, previous sensor mount designs were unable to accommodate the passage of so much material [14], [15]. Additionally, prior base station designs [12], [13] could not manage this amount of body material in the required weight specification (Table 1), and the resulting forces from the vine robot involved required a new analytical model to specify design requirements like motor capacity, material strength, and structural strength.

OUR CONTRIBUTION

To build on earlier vine robot systems for our large-scale application, we had to advance vine robot modeling, characterization, and design. First, we developed a model to analyze the effects, including pressure, gravity, friction, and tortuosity, that are unique to this scale and not considered in prior work. Second, we measured material and pneumatic properties at this unexplored scale to inform our analytical model. Finally, we used our model and analysis to develop a new vine robot body, base station, sensor mount, and control system to address the unique challenges of a vine robot at this scale.

MODELING AND CHARACTERIZATION

Modeling and experimental characterization were used to select a vine robot diameter and determine key operating parameters.

BUCKLING

We began by imposing buckling of the vine robot to be a failure case as this could lead to undesirable and unpredictable kinking behavior. We examined three possible buckling modes [16], [17], namely 1) transverse buckling, 2) crushing, and 3) axial buckling.

Transverse buckling occurs when an external moment is applied to the vine robot that overcomes the restorative internal moment. The restorative internal moment M_{cr} for a vine robot has been shown to be as follows [18]:

$$M_{cr} = PAR \quad (1)$$

where P is the internal pressure of the vine robot, A is its cross-sectional area, and R is its radius.

Crushing occurs when an axial compressive load, F_{crush} , exceeds the upward force provided by a vine robot's body pressure (its pressure P times its cross-sectional area A), and the vine robot crumples as follows:

$$F_{crush} = PA. \quad (2)$$

Lastly, axial buckling can occur prior to crushing if the vine robot, treated as an inflated beam, buckles similarly to a solid beam. This differs from transverse buckling and crushing where failure is caused by a loss of tension and subsequent buckling in the wall forming the inflated beam. Axial buckling of inflated beams has been modeled in prior works, including [19], and is predicted to occur when the axial load surpasses a critical force, F_{cr} , as follows:

$$F_{cr} = \frac{EI \frac{\pi^2}{L^2} (P + G\pi Rt)}{EI \frac{\pi^2}{L^2} + P + G\pi Rt} \quad (3)$$

where E is Young's modulus, I is the second moment of area of the vine robot body, L is the unconstrained length, G is the shear modulus, and t is the body thickness.

We can then solve the transverse buckling, crushing, and axial buckling equations to find the minimum pressure required to prevent each type of buckling. The maximum of these values is then used as a minimum bound for the vine robot body pressure. As the axial and transverse forces acting on the vine robot vary as the vine robot travels through the pipe (for instance, as the angle it makes with the pipe wall changes or as it grows outside the pipe), free body diagrams were constructed to model the force or moment terms in (1), (2), and (3) as functions of the vine robot's location in the pipe.

Buckling is also the primary consideration when modeling the lifting capability of a vine robot. As a growing vine robot can be modeled quasi-statically as a continuously lengthening inflated beam, (1), (2), and (3) can be used to find the maximum external moment or axial force that a vine robot can sustain from the environment or apply to a load, as has been demonstrated with vine robots in prior work [7], [16], [17].

VINE ROBOT GOVERNING EQUATIONS

Our growth and retraction models use [16] and [20] combined with task-specific elements to account for the tail's weight in vertical sections of pipe and the effect of an Ethernet cable being pulled through the vine robot body. First, for the vine robot to grow, P must be sufficiently great to satisfy the inequality as follows:

$$\frac{1}{2}PA \geq F_{\text{eversion}} + T_e + T_t + W_{\text{vertical}} + F_{\text{friction}} \quad (4)$$

where F_{eversion} is the material resistance to eversion, and F_{friction} represents the frictional forces on the vine robot tail as described in [20] and from interaction with the tip mount. T_e represents tension to pull the Ethernet cable, T_t represents the tail tension applied at the base station, and W_{vertical} represents the tail's weight in the vertical section.

Conversely, for the vine robot to retract, T_t must be sufficiently great to satisfy the inequality as follows:

$$T_t \geq \frac{1}{2}PA + F_{\text{inversion}} - T_e - W_{\text{vertical}} + F_{\text{friction}} \quad (5)$$

where $F_{\text{inversion}}$ is the material resistance to inversion as described in [16].

VELOCITY

As the requirements we were given specified a minimum time to grow and retract a set distance (Table 1), we had an effective velocity requirement to account for in our modeling. Prior vine robot literature notes that the material resistance to eversion F_{eversion} has a velocity dependence [20]. However, this velocity dependence is negligible for common vine robot operating speeds and materials relative to the static eversion resistance, and thus, we considered the eversion force to be a constant term.

A key operating parameter that is significantly impacted by the desired velocity is the volumetric flow rate of supplied air. As a vine robot lengthens, it must be continuously filled with air to maintain the desired growth pressure. At constant pressure, the required volumetric flow rate, V_f , supplied to a vine robot can be calculated as

$$V_f = v\pi R^2 \quad (6)$$

where v is the growth speed of the vine robot, and R is the radius of the vine robot. Since air compressors and fans are commonly characterized by the volumetric flow rate they provide as a function of discharge pressure, a desired vine robot body pressure and (6) can be used to select an adequate air supply source.

NUMERICAL MODEL

Using (1), (2), (3), (4), and (5), we developed a numerical simulation in MATLAB using experimentally measured coefficients to first determine the robot's required diameter and then its expected operating pressure and required retraction tension as it navigates the pipe. We used experimentally

measured coefficients of 0.34 for coefficient of friction and 0.5 N for material resistances to eversion and inversion. Based on findings from previous work, we took the material resistance to eversion and inversion to be independent of vine robot diameter [20]. These values were determined by growing and retracting vine robots while recording the tail tension load, pressure, length, and diameter, similar to the testing procedure described in [16, Sect. 2]. Vine robot body and tether material properties were also measured and are reported in the "Robot Body and Tether" section.

We first modeled the pressure required for vine robots of various diameters to grow without buckling as a function of their vertical height in the pipe system [Figure 5(a)]. For diameters less than the pipe diameter, the pressure required to meet our imposed no-buckling condition exceeded the burst pressure of the robot before it could exit the pipe. For a robot diameter equal to the pipe diameter (1 m), this is not seen because the pipe walls act to support the vine robot body. Although a smaller robot diameter that buckles and braces against the pipe wall may be feasible, for this work, we chose to eliminate buckling to improve the vine robot's controllability and video capture quality.

With our selection of a 1-m-diameter vine robot, we next found the minimum required pressure for growth and the minimum required tail tension at the base station for retraction. To find the required tension for retraction, we found the pressure needed to prevent buckling from (1), (2), and (3) and used it to solve (5) for tail tension at the base station. To determine the required pressure in growth, we solved (4) for pressure using an estimated friction force of 2 N for tail tension applied at the base station and validated that this pressure would prevent buckling. Figure 5(b) displays the magnitude of the forces resisting growth as a function of the vine robot's distance along the pipe, which in sum dictates the minimum required pressure in growth.

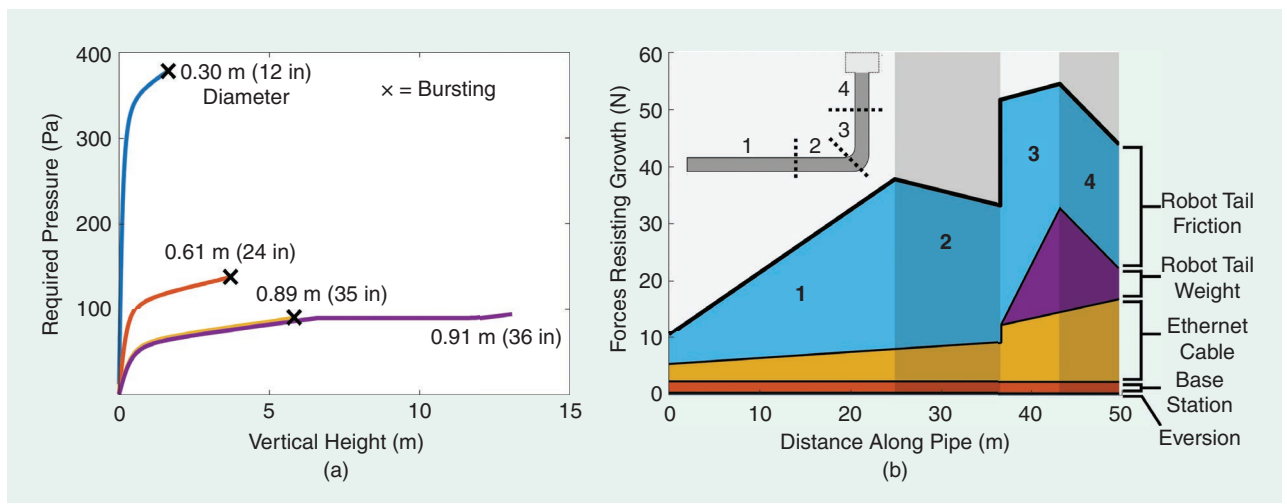


FIGURE 5. Selected models of vine robot operating parameters using governing equations in the "Modeling and Characterization" section. (a) Required pressure in growth without buckling for varying vine robot diameters in a 13-m (43-ft) vertical section. For the three smaller diameters, the plot lines end abruptly where the required pressure spikes and bursting would occur. (b) The forces resisting vine robot growth as described in (4). A description of the behavior in each portion of the pipe system is given in the "Numerical Model" section.

We identify four regimes of behavior as the vine robot grows through the pipe, highlighted in Figure 5(b). Note that the pressure required to grow is always proportional to the sum of the forces resisting growth, as described in (4).

- 1) The robot tail and Ethernet cable lengthen, increasing their respective linear frictions. The initial offsets are caused by constant friction from the Ethernet cable sliding through the base station and the vine robot tail sliding through the tip mount.
- 2) The tail material transitions from the robot body material to the significantly lighter tether material [Figure 4(b)], reducing robot tail friction even as the robot lengthens.
- 3) The robot rounds the turn, leading to a sharp increase in the tail and Ethernet resistive force due to capstan friction. As the vine robot grows vertically and pulls its tail and the Ethernet cable up the pipe, the robot tail and Ethernet cable weights increase.
- 4) The length of the inverted vine robot body material in the vertical section begins decreasing and is replaced by the lighter tether material, while the length and weight of the homogeneous Ethernet cable increase. The tail material in the horizontal pipe section is only a lighter tether material.

DESIGN

The primary purpose of our design was to create a vine robot that meets Bechtel's navigation and job-site deployability requirements. However, we also utilized Bechtel's inspection requirements to ensure that we developed a realistic design that could be built on in the future. For instance, by also developing a wired communication system, we ensured that our base station design could handle the communications wire without exceeding Bechtel's size and weight requirements.

Taken together, Bechtel's large-scale inspection task and corresponding constraints introduced unique design challenges that led to the need for a sensor mount capable of passing large volumes of vine robot body material through it, a compact and light base station capable of storing and rapidly inflating a large volume of material, and a joint wireless and wired communication system. The following sections highlight the main features of each of the robot's subassemblies, as seen in Figure 6.

ROBOT BODY AND TETHER

The vine robot body is made of a 0.08-mm-thick, 40-denier silicone-coated rip-stop nylon fabric (Rockywoods) chosen for its low weight, low friction, and high strength properties. Two sheets of fabric were bonded together with lap joints using silicone adhesive (Sil-poxy, Smooth-On), which yielded a final average density of 50.8 g/m². The robot tether is a sheet of 25.4 g/m² rip-stop nylon fabric, chosen instead of a cable to reduce tangling and spool diameter.

TIP MOUNT

A tip mount is used to keep a camera, light, and communications equipment at the distal end of the vine robot. Although not the primary focus of this work, we present this preliminary design to show that the use of a tip mount is possible at this scale. The key difference between our tip mount and preexisting designs is the contact condition between internal and external components. Preexisting designs use discrete contacts [14], [15], and we found that even when scaled up, our significantly increased vine robot diameter led to loose tail fabric jamming as it passed through the discrete contacts. To overcome this failure mode, we developed a continuous sliding contact between internal and external components to prevent jamming. We were able to combine this design with scaled-up versions of preexisting

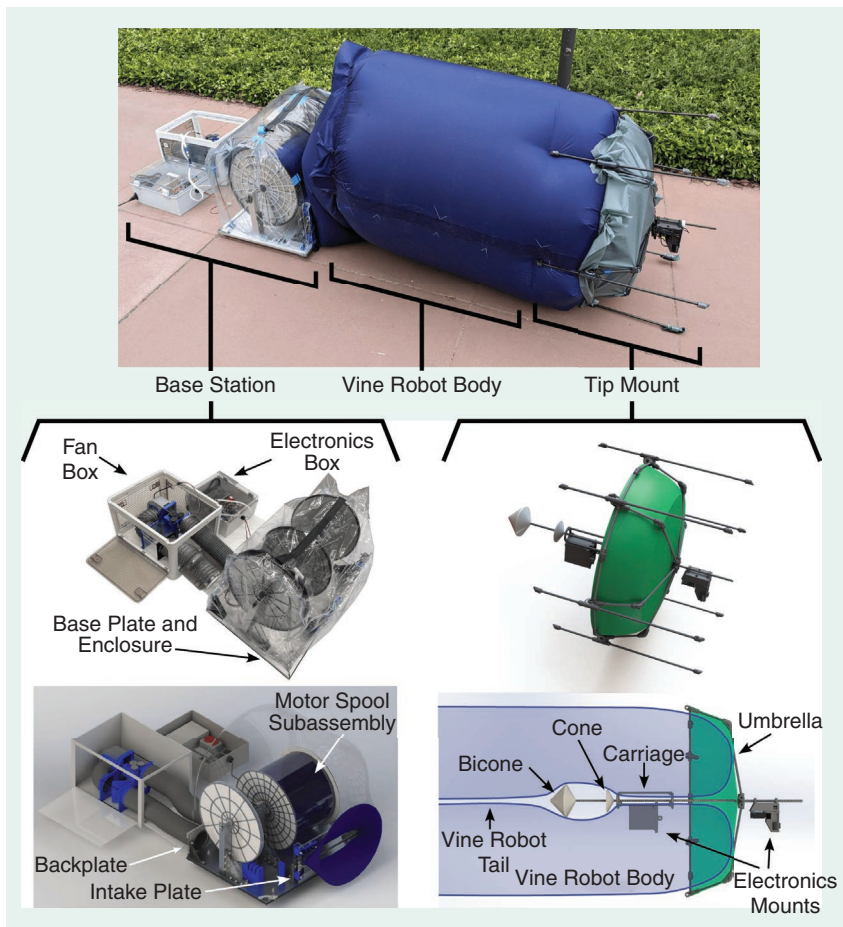


FIGURE 6. The deployed vine robot with its three main subsystems. Left: The base station consists of electromechanical components that support operation. Right: The tip mount carries the camera to provide a video stream of the pipe.

tip mount features to create the first tip mount for a vine robot whose meter-scale diameter is at least eight times larger than prior work [14]. In this preliminary development, we designed the tip mount only for straight growth; we believe the design of the tip mount can be readily modified to handle turns.

Our tip mount consists of an umbrella, a carriage, and two electronics mounts (Figure 6). The umbrella includes a fabric canopy attached to a carbon fiber tube frame that distributes the weight of the tip mount and keeps it at the tip of the vine robot body. Six pivoting carbon fiber tubes are attached around the fabric canopy as sliding surfaces and to guide the tip mount into the pipe system and over protruding weld lines. Additionally, a central carbon fiber rod connects the fabric canopy to an electronics mount located outside the vine robot body and to three 3D-printed cones engulfed by the vine robot body. Two of the three cones compose a bicone that helps guide the vine robot tail into the tip mount, while the third cone helps constrain the carriage.

The carriage is a hollow cylinder that fits around the central carbon fiber rod and fabric tail. The carriage provides a mounting location for the second electronics mount and can move only relative to the central carbon fiber rod by rotating around the rod's axis. The carriage is prevented from rotating or translating along any axis perpendicular to the central carbon fiber rod by the rod itself, while translation along the rod's axis is prevented by the cone on one side and the vine robot fabric on the other. The surface of the cone (an external component) and the annular end of the carriage (an internal component) create continuous contact, which allows a large amount of tail fabric to pass through the tip mount without jamming.

The tip mount operates as follows during robot operation. During growth, the body pressure forces the vine robot to evert, which pulls material through the tip mount. The everting fabric pushes the umbrella forward, which pulls the cone, carriage, and two electronics mounts with it (Figure 6). During retraction, the vine robot body inverts, pushing the carriage backward, which then pushes the cone and umbrella backward. In both growth and retraction, the tip mount remains at the front of the vine robot body and ensures that the camera has an unobstructed view.

BASE STATION

Our base station houses spooled robot material, an inflation fan, and communication interfaces to operate the robot. Base stations used in prior work [12], [13] would not meet Bechtel's size, weight, and time constraints without modifications. Our base station is made of soft inflatable materials rather than a rigid pressure vessel to reduce size and weight, uses a centrifugal fan rather than an air compressor to speed up vine robot inflation, and uses a gate to allow the fan to also speed up depressurization. The following sections describe the main assemblies comprising the base station.

MOTOR-SPOOL SUBASSEMBLY

We use a spool to compactly store unused vine robot fabric and control vine robot eversion. A second Ethernet spool stores the

Ethernet cable used for communications between the vine robot base and tip. A series of guide rollers ensure that the fabric and Ethernet cable wind over themselves uniformly.

Experimental tests and analytical modeling were used to model the radius of the fabric and Ethernet spools as functions of the length of the material spooled. This was then combined with our models for vine robot tail and Ethernet cable tension to select motors with sufficient torque and speed for each spool.

BASE PLATE AND ENCLOSURE

The aluminum-framed spool-motor assembly is fixed to a 3.175-mm-thick aluminum base plate using a set of 3D-printed and acrylic brackets. A vinyl sheet, fabricated into an open-faced bag using polyurethane glue (Item 1360694, Loctite Products), is clamped to the base plate by a set of four u-channels and latches. The vinyl bag and base plate create a lightweight airtight enclosure that can withstand the relatively low pressures required for our vine robot. An airtight zipper (8# TPU Zipper, TOPAZ) was attached to the top of the vinyl enclosure to provide easy access to the interior of the base station.

INTAKE AND BACKPLATE INTERFACES

The base plate and enclosure are connected to two subassemblies—the fan mechanism and the electronics box—via an interfacing backplate. The backplate consists of acrylic sheets that clamp to the vinyl enclosure with bolts and provide a mounting surface for the adapters used to facilitate the electrical and pneumatic connections between the base station's subassemblies.

The intake plate provides an opening in the enclosure for the spooled material to pass through as the robot everts. Similar to the backplate, it consists of two acrylic plates bolted to the vinyl enclosure, also allowing it to clamp the vine robot body to the base station enclosure.

FAN BOX AND ELECTRONICS BOX

The fan box and the electronics box were designed as modular components to meet Bechtel's weight and size requirements. To move large volumes of air at the relatively low pressure required by our large-diameter vine robot, the fan box is composed of a centrifugal fan (RBH1881B4, Pelonis) connected to a servo-driven gate mechanism used to rapidly switch between pressurizing and depressurizing the robot body. To power the base station, the electronics box converts ac power into dc using a 1,000-W power supply, and various buck converters were used to step the voltage down as required for electronic components. The electronics box also contains the hardware required to support communication between the user interface (UI) and the microcontrollers commanding the robot.

COMMUNICATIONS, ELECTRONICS, AND CONTROLS

The electronics and communications system controls all onboard sensors and actuators to enable operator-controller robot navigation and inspection (Figure 7). The communications system consists of a local Wi-Fi network with

routers at the base station and the tip mount connected via Ethernet. These routers act as network access points for sensors, microcontrollers, and the operator. Similar to vine robot designs like RoBoa [4], which transmit data from the tip to the base station, we utilized the wired-to-wireless hybrid communications architecture to run wires inside the vine robot body while collecting data from sensors outside the robot body.

A pressure sensor and a camera module are mounted at the tip of the vine robot. The pressure sensor is mounted on the tip mount inside the vine robot and attached to a Wi-Fi-enabled microcontroller (Raspberry Pi Pico W). The camera module is mounted on the tip mount outside the vine robot body and con-

sists of a single-board computer (Raspberry Pi 4) and a USB webcam (N980P, NexiGo). The Raspberry Pi streams the live camera feed to the user over the local network at low latency.

Inside the base station, current sensors monitor the fabric and Ethernet spool motor torques, and the ultrasonic and time-of-flight sensors monitor the spool diameters. We built a custom linear encoder consisting of an infrared sensor and dark lines marked on the Ethernet cable to measure the position of the vine robot's distal end.

A custom UI on the operator's computer displays these sensor readings and allows the operator to control the vine robot by sending commands to a Pico W microcontroller mounted in the electronics box. To modulate the pressure of

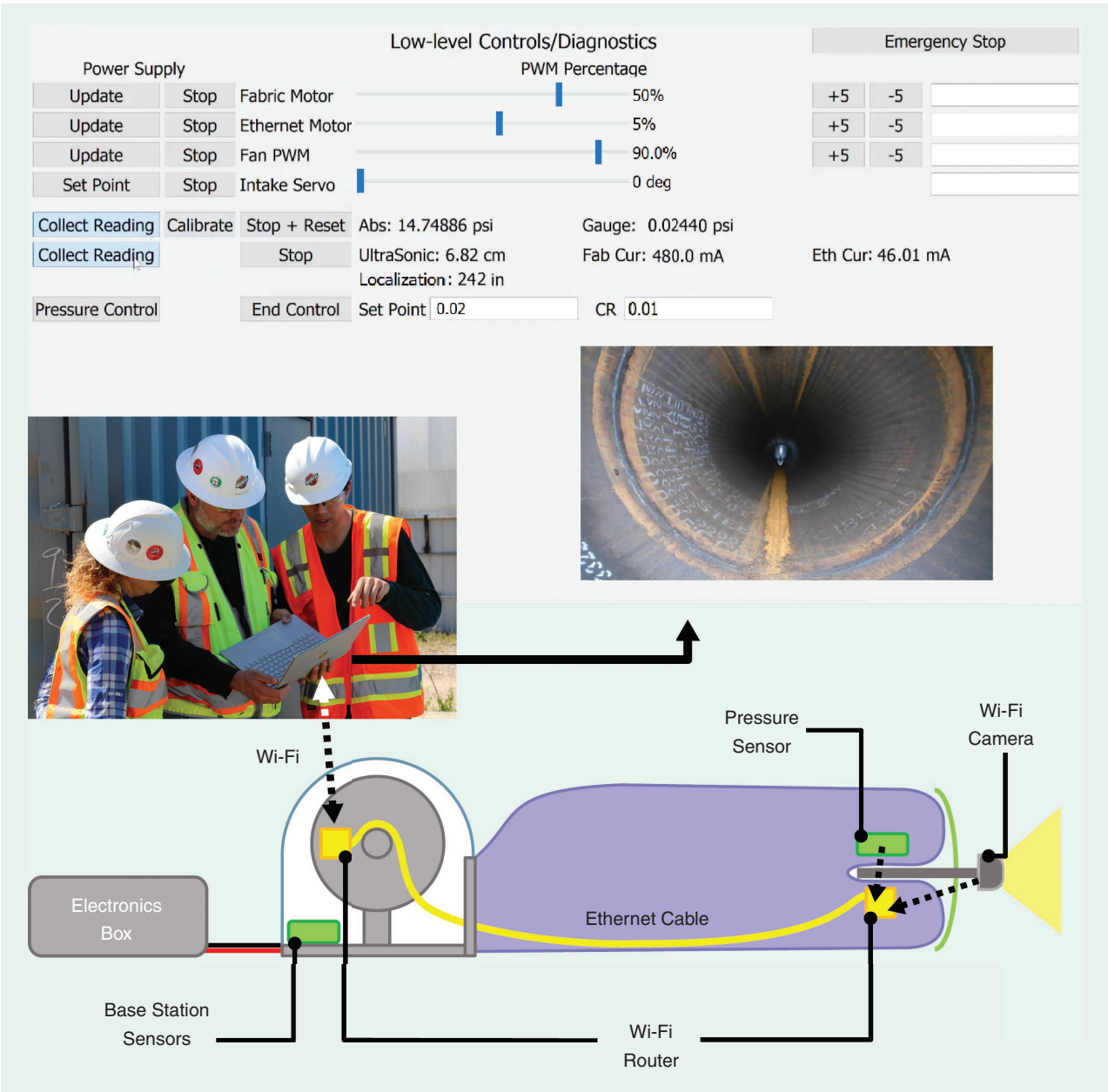


FIGURE 7. A diagram illustrating the robot's communication system. The UI provides a real-time video stream via a Wi-Fi connection with the vine robot. Note that the communication between the robot body and the base station is fully wired.

the vine robot, the UI allows the user to specify the nominal pressure target and the proportional gain. The control software then commands the fan pulse width modulation value and the fan box servo to reverse the airflow direction (as needed) to achieve the target pressure.

RESULTS

This section describes the findings from preliminary testing performed at the University of California, Santa Barbara (UCSB) as well as on-site testing performed at a Bechtel testing site in Houston, TX, USA.

PRELIMINARY TESTING AT UCSB

We successfully grew and retracted the robot to its full length of 33.5 m (110 ft) on a flat surface to validate its operation with and without the tip mount (Figure 8). We confirmed that our fan and motor settings worked well, but we identified a time-dependent drift in the pressure sensor readings of about 1.1 Pa/s. This was not significant enough to alter our control scheme but made collected data unreliable for model validation.

FIELD TESTING AT BECHTEL

The vine robot was shipped to a Bechtel testing site in Houston, TX, USA, where a steel pipe system was constructed as described in Figure 3. Due to manufacturing and cost constraints, the steel pipe was reduced from the original 37-m (120-ft) horizontal and 12-m (40-ft) vertical lengths to an 18-m (60-ft) horizontal section and a 6-m (20-ft) vertical section [Figure 9(a)].

Two runs of the robot were conducted. First, the vine robot was grown without the tip mount. The robot successfully navigated the entire pipe system in under 20 min and was able to grow higher than 3 m (10 ft) out of the pipe before buckling (Figure 1). This represents being able to grow into a large open tank with a much larger diameter than the entry pipe, a challenge for many types of inspection robots. Additionally, a 4-kg, 1.2-m by 1.2-m plywood board was placed over the pipe opening to simulate a pipe obstruction. The vine robot was able to successfully push the board away from the opening and continue growing [Figure 9(c)].

Following the successful test without the tip mount, the vine robot was grown through the pipe system with the tip

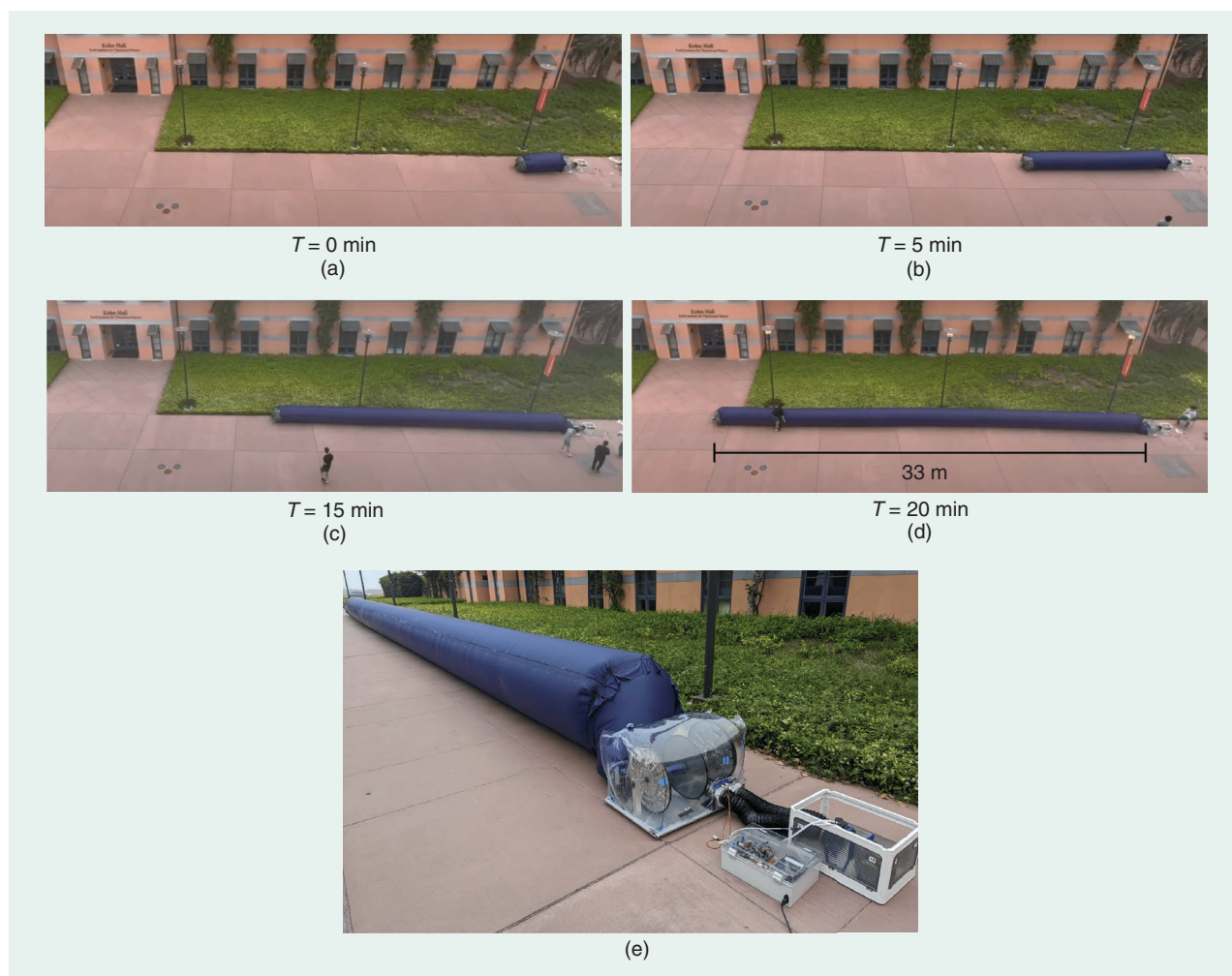


FIGURE 8. Results from the preliminary testing of the vine robot: (a)-(d) Time-stamped photos of the 33-m vine robot everting to its full length. (e) A photo illustrating the robot subsystems during operation.

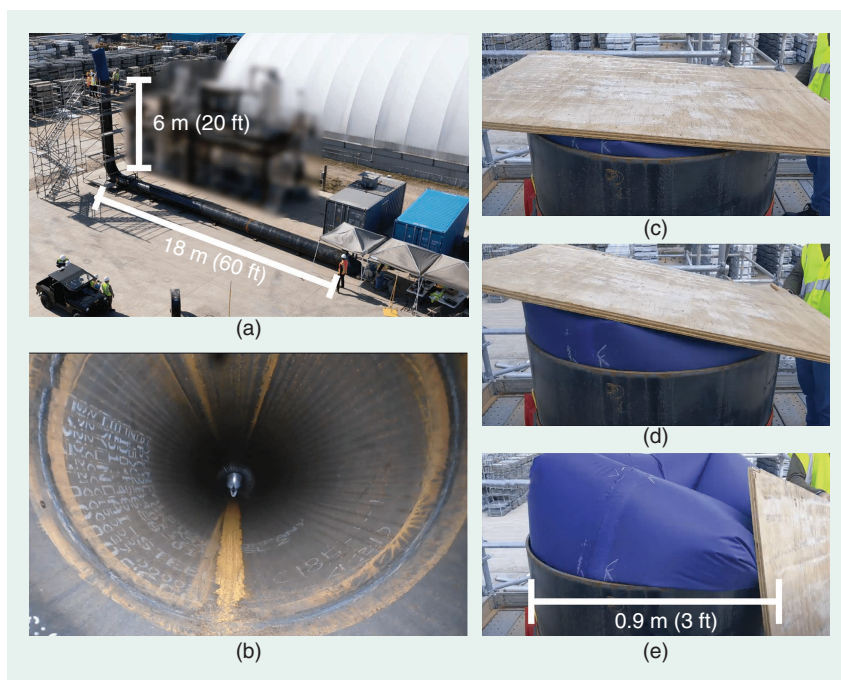


FIGURE 9. Results from field testing of the vine robot at the Bechtel test facility. (a) A photo illustrating the scale of the pipe system. The background of the image is blurred to protect confidential Bechtel Corporation equipment. (b) A video stream of the pipe provided by the robot. The robot navigated the weld lines visible in the image and was able to operate despite the presence of residual water in the pipe. (c)–(e) Photos highlighting the robot moving a plywood board before emerging from the pipe.

mount. Live video was captured of the vine robot's growth through the horizontal pipe section and displayed to the operators in real time via the UI [Figure 9(b)].

Finally, as a test to inform further development of the tip mount, the vine robot was grown through the elbow in the pipe with the tip mount in place. As the vine robot grew forward into the elbow, the umbrella was pivoted down into the pipe rather than following the contour of the elbow, causing the robot to stall. We believe that this failure mode could be prevented with minor modifications, as discussed in the “[Discussion and Future Work](#)” section.

With respect to Bechtel's other requirements, the base station was the heaviest and largest component of the deployed robot, with a weight and maximum dimension of 22 kg and 0.8 m, respectively, but it met the desired weight and linear dimension targets. Throughout testing, the robot was also unaffected by environmental factors like rust, dirt, residual standing water in the pipe system, and high temperatures, highlighting the robustness of the vine robot in industrial settings.

DISCUSSION AND FUTURE WORK

We presented a large-scale field-deployable vine robot system capable of navigating a real-world piping system scenario. This work serves as a first step toward addressing a pipe system inspection challenge posed to us by the engineering and construction company Bechtel. Our vine robot design met Bechtel's size, weight, and speed constraints and demonstrated the ability

of a tethered robot to traverse a long curved pipe system with a large diameter and an opening into an unconstrained space.

The unique working principle of the vine robot proved advantageous for industrial-scale pipe navigation. The vine robot's pressure-driven eversion allowed it to generate large propulsion forces to pull a tether and equipment through the pipe, while its plant-like growth allowed it to create a stable body to support it in the vertical and large increase in diameter pipe sections. We also demonstrated that these benefits persist for a vine robot multiple times larger than the previous vine robots, and we addressed multiple modeling and design challenges encountered when attempting to scale up vine robots.

Our vine robot grew and retracted successfully to its full length with and without a tip mount during preliminary testing in free space and through the entire pipe system without the tip mount. However, the tip mount did not successfully pass through the elbow

of the pipe system. We believe that the tip mount was not adequately guided through the elbow bend by the compliant vine robot. This could be addressed by adding protruding elements to the tip mount exterior to force it to follow the pipe geometry or by extending the umbrella backwards to better constrain it to the vine robot body.

Additionally, a key choice we made was the conservative decision to consider buckling a failure condition for the vine robot. However, a vine robot may be able to buckle and brace itself against the environment in a stable manner. This could allow vine robots of smaller diameters to be used, thereby reducing the weight, size, and cost of a given vine robot system and potentially allowing easier passage through tight corners with a tip mount.

In our future work, we aim to build on the advances made to meet Bechtel's navigation and field-deployability requirements as well as what we have learned toward adding sensing capabilities to develop a vine robot that completes Bechtel's pipe inspection task. Additionally, we developed a new model for vine robot growth and retraction, some of which is shown in Figure 5(b). While individual components of our model have been validated with small-scale vine robots [13], [16], [17], [20], we aim to conduct further experimental testing to validate our full model at large scales through the use of a representative pipe system environment and sensitive pressure gauges that can detect the small pressures used, even in the presence of small leaks or temperature changes. We also aim to investigate applying large-scale vine robots for other

industrial facility tasks. The propulsion capabilities of large-scale vine robots, along with their compliance, robustness to environmental factors, ability to apply large forces to the environment, and self-supporting capabilities, may be useful for applications involving storage tanks, machinery, or chemical distillation towers.

Prior vine robot research on active steering methods [7], predicting environmental interaction [17], and passing through constrictions [14] can also be leveraged for more complex industrial asset inspections, such as those requiring the vine robot to navigate an open chamber to exit routes of varying diameter. While this work was not the focus of this proof of concept, we aim to integrate these capabilities in future work with large-scale vine robots to increase their usefulness for industrial pipe system inspection and beyond.

ACKNOWLEDGMENT

We thank Keith Churchill, Charles Bailey, and Katherine Toscana from the Bechtel Corporation for their support of this work; John Chen, Nate Olivo, and Rajveer Oberoi at UCSB for their contributions to the design and testing of the vine robot; and Dr. Trevor Marks at UCSB for his assistance with the electronics systems. This work was supported in part by NSF Grant 1944816, in part by Bechtel Corporation, in part by the UC Santa Barbara Office of Undergraduate Research and Creative Activities, and in part by the California NanoSystems Institute Innovation Award. The authors also acknowledge the use of the Microfluidics Laboratory (Innovation Workshop) within the California NanoSystems Institute, supported by the University of California, Santa Barbara and the University of California, Office of the President.

AUTHORS

William E. Heap, Department of Mechanical Engineering, Stanford University, Stanford, CA 94305 USA. E-mail: wheap@stanford.edu.

Steven Man, Robotics Institute, Carnegie Mellon University, Pittsburgh, PA 15213 USA. E-mail: stevenwman@cmu.edu.

Vedad Bassari, Department of Mechanical Engineering, University of California, Santa Barbara, Santa Barbara, CA 93106 USA. E-mail: vedad@ucsb.edu.

Steven Nguyen, Department of Mechanical and Aerospace Engineering, University of California, San Diego, La Jolla, CA 92093 USA. E-mail: stn030@ucsd.edu.

Elvy B. Yao, College of Engineering, University of California, Santa Barbara, Santa Barbara, CA 93106 USA. E-mail: eyao@ucsb.edu.

Neel A. Tripathi, College of Engineering, University of California, Santa Barbara, Santa Barbara, CA 93106 USA. E-mail: ntripathi@ucsb.edu.

Nicholas D. Naclerio, Department of Mechanical Engineering, University of California, Santa Barbara, Santa Barbara, CA 93106 USA. E-mail: nnaclerio@ucsb.edu.

Elliot W. Hawkes, Department of Mechanical Engineering, University of California, Santa Barbara, Santa Barbara, CA 93106 USA. E-mail: ewhawkes@ucsb.edu.

REFERENCES

- [1] D. Lattanzi and G. Miller, "Review of robotic infrastructure inspection systems," *J. Infrastruct. Syst.*, vol. 23, no. 3, 2017, Art. no. 04017004, doi: [10.1061/\(ASCE\)IS.1943-555X.0000353](#).
- [2] NFPA-59a, *Production, Storage, and Handling of Liquefied Natural Gas (LNG)*. Quincy, MA, USA: National Fire Protection Association (NFPA) (Latest Edition), 1990.
- [3] A. Verma, A. Kaiwart, N. D. Dubey, F. Naseer, and S. Pradhan, "A review on various types of in-pipe inspection robot," *Mater. Today: Proc.*, vol. 50, pp. 1425–1434, Feb. 2022, doi: [10.1016/j.matpr.2021.08.335](#).
- [4] P. A. der Maur et al., "RoBoa: Construction and evaluation of a steerable vine robot for search and rescue applications," in *Proc. IEEE 4th Int. Conf. Soft Robot. (RoboSoft)*, 2021, pp. 15–20, doi: [10.1109/RoboSoft51838.2021.9479192](#).
- [5] M. Takeichi, K. Suzumori, G. Endo, and H. Nabae, "Development of a 20-m-long giacometti arm with balloon body based on kinematic model with air resistance," in *Proc. IEEE/RSJ Int. Conf. Intell. Robots Syst. (IROS)*, Piscataway, NJ, USA: IEEE Press, 2017, pp. 2710–2716, doi: [10.1109/IROS.2017.8206097](#).
- [6] T. Waters, V. Putz-Anderson, and A. Garg, "Applications manual for the revised NIOSH lifting equation." [Online]. Available: <https://www.cdc.gov/niosh/docs/94-110/>
- [7] L. H. Blumenschein, M. M. Coad, D. A. Haggerty, A. M. Okamura, and E. W. Hawkes, "Design, modeling, control, and application of everted vine robots," *Front. Rob. AI*, vol. 7, Nov. 2020, Art. no. 548266, doi: [10.3389/frobt.2020.548266](#).
- [8] D. Mishima, T. Aoki, and S. Hirose, *Development of Pneumatically Controlled Expandable Arm for Search in the Environment With Tight Access*. Berlin, Germany: Springer-Verlag, 2006.
- [9] H. Tsukagoshi, N. Arai, I. Kiryu, and A. Kitagawa, "Tip growing actuator with the hose-like structure aiming for inspection on narrow terrain," *Int. J. Autom. Technol.*, vol. 5, no. 4, pp. 516–522, 2011, doi: [10.20965/ijat.2011.p0516](#).
- [10] E. W. Hawkes, L. H. Blumenschein, J. D. Greer, and A. M. Okamura, "A soft robot that navigates its environment through growth," *Sci. Robot.*, vol. 2, no. 8, 2017, Art. no. eaan3028, doi: [10.1126/scirobotics.aan3028](#).
- [11] J. D. Greer, T. K. Morimoto, A. M. Okamura, and E. W. Hawkes, "A soft, steerable continuum robot that grows via tip extension," *Soft Robot.*, vol. 6, no. 1, pp. 95–108, 2019, doi: [10.1089/soro.2018.0034](#).
- [12] M. M. Coad et al., "Vine robots," *IEEE Robot. Autom. Mag.*, vol. 27, no. 3, pp. 120–132, Sep. 2020, doi: [10.1109/MRA.2019.2947538](#).
- [13] J. Luong et al., "Eversion and retraction of a soft robot towards the exploration of coral reefs," in *Proc. 2nd IEEE Int. Conf. Soft Robot. (RoboSoft)*, 2019, pp. 801–807, doi: [10.1109/ROBOSOFT.2019.8722730](#).
- [14] W. E. Heap, N. D. Naclerio, M. M. Coad, S.-G. Jeong, and E. W. Hawkes, "Soft retraction device and internal camera mount for everted vine robots," in *Proc. IEEE/RSJ Int. Conf. Intell. Robots Syst. (IROS)*, 2021, pp. 4982–4988, doi: [10.1109/IROS51168.2021.9636697](#).
- [15] S.-G. Jeong et al., "A tip mount for transporting sensors and tools using soft growing robots," in *Proc. IEEE/RSJ Int. Conf. Intell. Robots Syst. (IROS)*, pp. 8781–8788, 2019, doi: [10.1109/IROS45743.2020.9340950](#).
- [16] M. M. Coad, R. P. Thomasson, L. H. Blumenschein, N. S. Usevitch, E. W. Hawkes, and A. M. Okamura, "Retraction of soft growing robots without buckling," *IEEE Robot. Autom. Lett.*, vol. 5, no. 2, pp. 2115–2122, Apr. 2020, doi: [10.1109/LRA.2020.2970629](#).
- [17] D. A. Haggerty, N. D. Naclerio, and E. W. Hawkes, "Characterizing environmental interactions for soft growing robots," in *Proc. IEEE/RSJ Int. Conf. Intell. Robots Syst. (IROS)*, Piscataway, NJ, USA: IEEE Press, 2019, pp. 3335–3342, doi: [10.1109/IROS40897.2019.8968137](#).
- [18] Z. M. Hammond, N. S. Usevitch, E. W. Hawkes, and S. Follmer, "Pneumatic reel actuator: Design, modeling, and implementation," in *Proc. IEEE Int. Conf. Robot. Automat. (ICRA)*, 2017, pp. 626–633, doi: [10.1109/ICRA.2017.7989078](#).
- [19] W. Fichter, U. S. N. Aeronautics, S. Administration, and L. R. Center, *A Theory for Inflated Thin-Wall Cylindrical Beams*, vol. 3466. Washington, DC, USA: National Aeronautics and Space Administration, 1966.
- [20] L. H. Blumenschein, A. M. Okamura, and E. W. Hawkes, "Modeling of bioinspired apical extension in a soft robot," in *Biomimetic and Biohybrid Systems*, M. Mangan, M. Cutkosky, A. Mura, P. F. Verschure, T. Prescott, and N. Lepora, Eds., Cham, Switzerland: Springer-Verlag, 2017, pp. 522–531.

